GEOCHEMISTRY AND GEOCHRONOLOGY OF SURFICIAL ACRE BASIN SEDIMENTS (WESTERN AMAZONIA): KEY INFORMATION FOR CLIMATE RECONSTRUCTION.

B. I. Kronberg (1)
R. E. Benchimol (2)

ABSTRACT

Geochemical and geochronological analyses of samples of surficial Acre Basin sediments and fossils indicate an extensive fluvial-lacustrine system, occupying this region, desiccated slowly during the last glacial cycle (LGC). This research documents direct evidence for aridity in western Amazonia during the LGC and is important in establishing boundary conditions for LGC climate models as well as in correlating marine and continental (LGC) climate conditions.

INTRODUCTION

The Acre Basin is the westernmost subbasin of Amazonia and is geologically defined by the Iquitos Arch, which separates it from the upper Amazon Basin (Figure 1a; Asmus & Porto, 1972). Drill core profiles through the upper 5 km of the basin indicate that the Acre Basin was transformed during the Andean orogeny from a continental margin to an intracontinental setting (Miura, 1972). The surficial sediments of the basin investigated in this study, are considered to be representative of the Solimoes Formation, characterized by clay sediments, in which are intercalated sand banks, lignitic lenses, gypsum veins and calcareous concretions (Rego, 1930; Santos, 1984).

This study documents detailed geochemical data from a series of Acre Basin sediment samples collected along the upper Purus and lower Acre Rivers (Figures 1a, 1b) with the intention of achieving a better understanding of the geological history of the Acre Basin. Also, documented here are the first AMS (accelerator mass spectrometry) radiocarbon dates for Western Amazonia.

EXPERIMENTAL

Sample Collection and Description

In 1986 samples were collected at 11 sites along the upper Purus River in the vicinity of Boca do Acre (Figure 1b). In 1989 sediment samples were collected from a site on the lower Acre River at which scientists from the University of Acre had found virtually complete skeletons of reptilian fauna (Figure 1a). This finding indicates these sediments have not been significantly reworked since deposition.

[1] Lakehead University Thunder Bay, Canada P7B 5E1.
[2] Federal University of Amazonas 69 000 Manaus Brasil.

Acta Amazonica, 22 (1): 51 - 69. 1992.

Fig. 1a - Sketch map showing relative locations of Purus and Acre River Sites

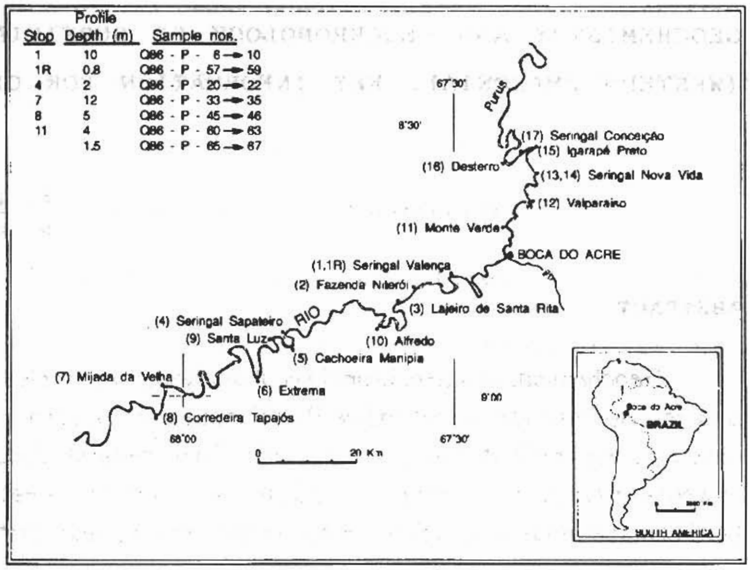

Fig. 1b - Sketch map of Purus River Sites

Table 1
Sample Descriptions

a) Purus River Sites

Site	Sample	Description
1	Q86 P-6 (top)	
	P-7	
	P-8	10 m profile of riverbak sediments
	P-9	
	P-10	
	P-11	sediment enclosing
	P-12,12A	carbonate concretions found at water level
	P-13 (top) P-14 P-15	1 m profile through clay sediment to accompany detailed collection for palynology studies
2	P-16	sample from riverbank (mid-profile)
3	P-17	conglomerate sample from "lajeiro"
4	Q86 P-18A	pyrite sample
	P-18B	pyritized wood sample dated at >25,000 a B.P.
	P-18C	sample of sediment enclosing
	P-19	carbonate (aragonite) concretion
	P-20 (top)	
	P-21	2 m profile through clay sediments
	P-22	
	P-23	clay sample
	P-24	carbonaceous clay sample
5	P-25	sediment samples from "lajeiro"
	P-27	

Cont.

Site	Sample	Description
7	Q86 P-30	gypsum-rich sample
	P-31	sediment enclosing P-30
	P-32	sample of "indurated" sediment crust
	P-33	
	P-34	1.2 m profile through heavy clays for palynology studies
	P-36	
7	Q86 P-37	calcite carbonate apatite concretion
	P-38	organic-rich sample
	P-39	gypsum rich sample
	P-40	sample of sediment enclosing organic-rich unit containing
	P-43	tree trunk dated at 45,180 a B.P.
8	P-44	sediment sample from lowr riverbank
	P-45	sediments from upper (recent) sediments
	P-46a,b	
9	Q86 P-49	sample of "conglomerate"
10	P-51	sediment enclosing samples of wood, shells, fish bones and
	P-56	seed dated at 32,160 a B.P.
	P-53	sample of overlying sediments
IR	P-57 P-58	0.8 m profile through heavy clays for palynology studies
	P-59	
11	Q86 P-60 (top)	
	P-61 P-62	4 m profile through sediment 20 m above water level
	P-63	
	P-65	
	P-66a P-66b	1.5 m profile through sediment terrace ~2 m above water level
	P-67a	
17	Q86 P-69	sample of "Varzea" sediment
15	Q86 P-68	wood sample (45,190 a BP) entrained in sediment
	P-72	sample of recently deposited sediment
	P-74	sample of sandstone

Most samples are from a series of profiles through river bank sediments (Sites 1, 1R, 4, 7, 7, 11; Table 1) on the upper Purus River. Samples from a profile on the lower Acre River (~200 km south of the Purus River sites) provide an assessment of the geochemical and geochronological similarities between sediments from the 2 locations. The clay-sized material (Figure 2a) predominant in these samples is considered to have been laid down in a lake bed depositional environment. Calcium carbonate ($CaCO_3$) concretions (Figure 2b) and gypsum ($CaSO_4.2H_2O$) were commonly intercalated with the clay sediments. A prominent lignitic sediment lense was found at site 7 (Purus River).

b) Acre River Site

Site	Sample	Description
1	Q89 A-1 (bottom)	4 m profile of clay (lake bed) sediments beginning from water level
	A-2	
	A-3	
	A-4	
	A-5	
	A-6	recent sediment deposited over clay sediments
	Q89 A-B	reptilian bone from uppermost clay sediment layer (Q89 A-5)
	Q89 A-Ca	an aragonite concretion entrained in sediment ~4 m below uppermost clay sediment
	AMM-89	wood entrained in sediment ~4 m below uppermost clay sediment

Sample Analysis

Major and minor element compositions were determined using X-ray fluorescence (Table 2a, 3a) and inductively coupled plasma (ICP) optical emission spectrometry (Table 2b, 3b). X-ray diffraction (XRD) was used to determine the major minerals in each sample.

AMS radiocarbon age dates were determined for samples of carbonate concretions and biological materials entrained in sediments (Table 4a). ^{13}C, ^{18}O and $^{87}Sr/^{86}Sr$ isotopic ratios were determined in samples of carbonate concretions (Table 4b).

Mineral and Major Element Compositions

The clastic sediment samples are composed mainly of oxides of Al and Si (Tables 2a, 2b) bound mainly as quartz and kaolinite. Complex clays, feldspar, hematite, goethite and calcite are trace constituents. Siderite, aragonite and gypsum are also common trace constituents, but, in some samples, these are major phases. Gypsum appears both as selenitic gypsum and as elongated crystal aggregates up to 3.5 m in length infilling sediment cracks (Figure 2c). Traces of fluorapatite were observed in some samples and one carbonate concretion contained mainly calcite and carbonate apatite.

The extent of chemical weathering in the clastic sediment samples was quantified using a ''chemical index of alteration'', CIA, which is based on a feldspar weathering model (Kronberg & Nesbitt, 1981; Kronberg **et al.**, 1986) and calculated using the following ratio of oxide concentrations expressed in moles:

$$CIA = [Al_2O_3/(Al_2O_3 + CaO^* + Na_2O + K_2O)] \times 100,$$

where CaO* represents calcium associated only with silicate phases. CIA values range from ~50 for average upper crust, to ~100 for the most highly weathered continental materials. The assumption is that continental crustal materials with similar source regions and chemical weathering histories would have similar CIA values.

Generally high CIA values (CIA > 80; Tables 3a, 3b) for the sediment samples collected for this study indicate that these sediments have undergone intense chemical weathering. Most values for the surficial

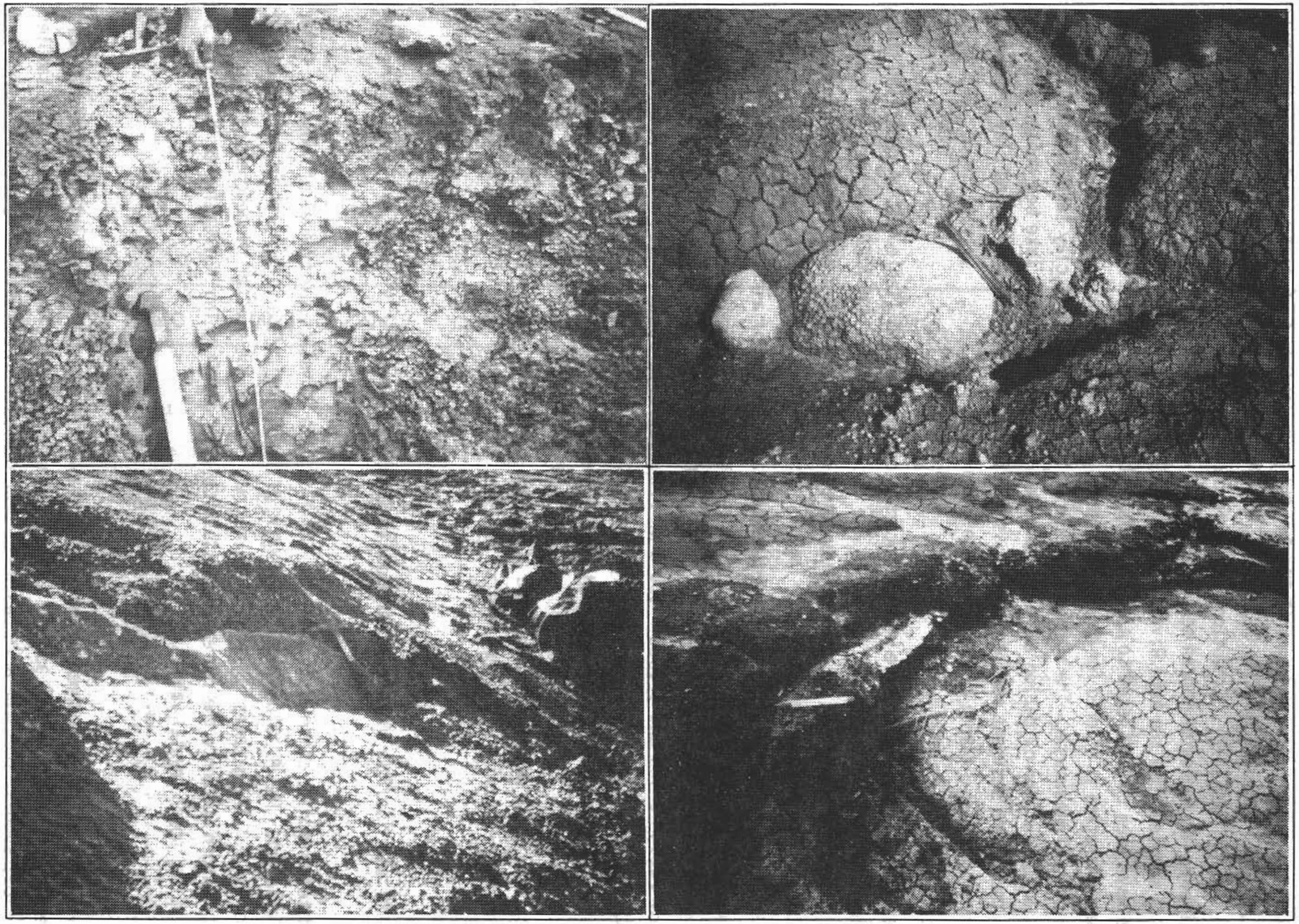

Fig. 2a - (Upper left) - Profile of clay lake bed sediments.

Fig. 2b - (Upper right) - Calcium carbonate (aragonite) concretions embedded in lake sediments.

Fig. 2c - (lower left) - Vertical rows of elongated gypsum crystals infilling sediment cracks.

Fig. 2d - (lower right) - Tree trunk (radiocarbon ae 45,180 ± 490 a BP, sample Q86-P-43) protruding from carbon-rich clay sediment layer.

sediment samples representing the lakebed environment are clustered around the mid-eighties indicating that the sediments have similar chemical westhering histories and source areas.

Minor Elements

In general minor element concentrations (Table 3a, 3b) are within a factor of two of their crustal abundances (S, 340; V, 136; Cr, 122; Co, 29; Cu, 68; Zn, 76; Rb, 78; Sr, 384; Y, 31; Zr, 162; Nb, 20; Mo, 1.2; Ba, 390; Pb, 13; Fairbridge, 1972). Exceptions are Zr in the most intensely chemically weathered samples at site 11 (Purus River), in samples of modern sediments (Q86-P-45, 69, 72) and in ''conglomerate'' samples (Q86-P-16, 17). S in samples from the Acre River site is concentrated 20-40 fold relative to its crustal abundance. S could have been concentrated to these levels by biorganic processes operating on the active lake floor. A similar explanation is offered for Mo, which also has a strong bioaffinity, being 2-7 times enriched with respect to its crustal abundance. The strong decrease in S in the uppermost clay lake bed sample (89-A-5) may be indicative of sulphur oxidation and incorporation into gypsum as the lake bed desiccated. At the Acre River site the modern sediment sample (89-A-6) is distinguished from the underlying clay sediments by its relatively lower (up to 2-3 times) concentrations of minor elements.

Geochronology

Three samples from the Acre River site were radiocarbon dated using AMS (Table 4a). A reptilian bone sample fron the uppermost lake bed sediments have an age date of 23,950 ± 420 A BP. Other radiocarbon dates at this site are from a sample of an aragonite concretion (49,110 ± 900 a BP) and a sample of wood (41,850 ± 490) located ~4 m below the uppermost lakebed sediments.

A wood sample (Kromberg - 1) entrained in sediments at the bottom of a river bank within the city limits of Rio Branco gave a radiocarbon date of 11,870 ± 70 a BP.

Two other reptilian bone samples (Kronber - 2, 3) collected during excursions prior to 1986 gave radiocarbon ages of 24,130 ± 330 and 12,060 ± 150 a BP respectively.

The remaining age dates are from sites (4, 7, 10, 15) along the Purus River. At site 4 the oldest age date (53,270 ± 1,850 a BP) in this study was obtained from an aragonite concretion. A pyritized wood sample also collected at site 4 gave a radiocarbon age of > 25,000 a BP. At site 7 a fossil tree trunk (Figure 2d) protruding from a lignitic lense was radiocarbon dated at ~45,180 ± 690 a BP. A fossil seed (site 10) entrained in clay sediment and another fossil wood sample (site 15) have radiocarbon ages of 32,160 ± 230 and 45,190 ± 830 a BP respectively.

^{13}C, ^{18}O and $^{87}Sr/^{86}Sr$ Values in Aragonite Concretions

In the age dated aragonite concretions (89-A-Ca, Q86-P-19) the ^{18}O values are typical of those for fresh water carbonates (Table 4b). The ^{13}C values are consistent with the biological participation in the nucleation and precipitation of $CaCO_3$. The greater ^{13}C range of values may reflect the greater biogeochemical mobility of carbon relative to oxygen and hence the increased possibilities for partitioning ^{12}C relative to ^{13}C. $^{87}Sr/^{87}Sr$ isotope ratios are typical upper crustal values.

DISCUSSION

The extensive distribution of sediments dominated by clay-sized material throughout the surficial Acre Basin sediments (Rego, 1930; Santos, 1984) as well as the dominance of thick clay units in drill core samples (Kronberg **et al.**, 1989) suggest that the Acre Basin has been occupied by lacustrine systems. Clay-sized material would be carried to offshore lacustrine waters from which it would flocculate and deposit slowly, forming uniform clay units, as observed in the field and drill core profiles.

Table 2(a)
Major Element Oxide Concentrations (Weight %)
(Purus River Sites)

Sample	Na_2O	MgO	Al_2O_3	SiO_2	P_2O_5	K_2O	CaO	TiO_2	Fe_2O_3	MnO	LOI
Site 1											
Q86-P-6	0.1	0.9	13.5	66.7	0.2	1.8	0.5	0.8	6.8	0.3	8.2
Q86-P-7	0.2	1.0	19.5	53.6	0.2	2.3	2.8	0.9	5.2	0.03	14.2
Q86-P-8	0.9	0.5	8.3	78.7	0.1	1.7	0.6	0.9	3.4	0.1	4.1
Q86-P-9	0.2	1.5	18.3	57.0	0.2	2.5	1.2	1.0	6.4	0.1	11.8
Q86-P-10	0.2	1.3	19.5	56.3	0.3	2.3	1.2	1.0	4.8	0.03	13.2
Q86-P-11	0.2	1.3	19.8	55.7	0.2	2.5	1.1	1.0	5.0	0.04	13.1
Q86-P-12	0.1	0.3	7.2	30.5	0.3	1.1	0.5	0.6	51.1	0.2	7.9
Q86-P-12A	<0.01	0.6	6.9	22.0	0.1	0.8	35.0	0.3	2.8	0.03	31.3
Q86-P-13	0.2	1.5	19.2	56.0	0.3	2.3	1.3	0.9	6.0	0.04	12.2
Q86-P-14	0.2	1.5	19.8	57.8	0.1	2.4	1.3	1.0	4.1	0.03	11.8
Q86-P-15	0.2	1.4	19.3	54.8	0.2	2.3	1.4	0.9	7.0	0.1	12.8
Site 2											
Q86-P-16	<0.01	0.2	7.9	55.2	0.1	0.9	0.1	0.9	27.4	0.04	7.5

cont.

Sample	Na_2O	MgO	Al_2O_3	SiO_2	P_2O_5	K_2O	CaO	TiO_2	Fe_2O_3	MnO	LOI
Site 3											
Q86-P-17	0.2	0.2	3.1	50.0	0.7	0.8	0.5	0.6	36.0	1.4	6.5
Site 4											
Q86-P-18C	0.2	1.4	18.4	58.7	0.1	2.7	1.1	0.9	5.7	0.04	10.8
Q86-P-19	<0.01	0.1	0.9	3.0	0.1	0.1	53.3	0.1	0.4	<0.01	41.0
Q86-P-20	0.2	0.2	13.5	68.5	0.1	1.4	0.1	1.0	7.2	0.03	7.3
Q86-P-21	0.1	0.4	16.8	71.3	0.1	1.6	0.1	1.0	1.6	0.02	6.4
Q86-P-22	0.1	0.3	14.0	73.1	0.1	1.9	0.1	1.0	4.0	0.02	5.2
Q86-P-23	0.2	1.3	18.1	59.8	0.2	2.6	1.0	0.9	4.8	0.03	11.3
Q86-P-24	0.2	1.2	19.7	50.0	0.1	2.3	0.9	0.9	3.8	0.02	20.7
Site 5											
Q86-P-25	0.2	0.1	3.2	49.4	0.4	0.8	28.3	0.4	28.3	1.4	14.8
Q86-P-27	<0.01	0.2	2.0	7.1	0.5	0.4	2.2	0.2	57.0	1.2	29.4
Site 7											
Q86-P-30	<0.01	0.2	3.6	11.7	0.1	0.5	27.7	0.2	1.0	<0.01	21.3
Q86-P-31	0.1	1.1	17.6	57.4	0.1	2.3	1.9	1.9	6.3	0.04	12.0
Q86-P-32	0.1	0.2	8.4	61.5	0.4	1.2	0.3	0.8	19.2	0.8	7.1

cont.

Sample	Na_2O	MgO	Al_2O_3	SiO_2	P_2O_5	K_2O	CaO	TiO_2	Fe_2O_3	MnO	LOI
Q86-P-33	0.2	1.5	18.6	57.0	0.2	2.4	1.5	0.9	5.1	0.03	12.4
Q86-P-34	0.2	1.6	18.0	57.3	0.4	2.5	1.5	0.9	5.5	0.1	11.5
Q86-P-35	0.2	1.1	18.8	52.5	0.1	2.2	2.5	0.9	7.0	0.03	14.0
Q86-P-36	0.2	1.1	17.9	58.9	0.1	2.3	0.9	1.0	6.4	0.04	10.7
Q86-P-37	0.3	0.7	7.7	25.7	14.9	1.1	29.9	0.4	2.6	0.9	15.2
Q86-P-40	0.1	1.1	14.2	41.5	0.1	1.8	1.0	0.8	7.9	0.04	31.3
Site 8											
Q86-P-44	0.8	1.1	14.0	67.9	0.07	1.9	0.07	0.9	4.8	0.03	8.0
Q86-P-45	0.8	0.3	5.8	83.7	0.1	1.3	0.5	1.0	2.9	0.1	2.5
Q86-P-46a	0.4	0.2	4.0	73.4	0.2	1.2	0.5	0.6	14.5	0.7	4.3
Q86-P-46b	0.1	0.2	1.9	11.2	0.6	0.3	2.7	0.2	52.8	2.9	27.3
Site 9											
Q86-P-49	0.1	1.2	11.4	47.2	2.2	2.0	3.7	0.7	18.1	0.9	12.4
Site 10											
Q86-P-51	0.2	1.1	17.8	51.3	0.9	2.4	2.2	0.9	7.9	0.1	14.6
Q86-P-53	0.2	0.9	15.7	53.1	1.2	2.3	3.6	0.8	8.7	0.1	12.5

CONT.

Sample	Na_2O	MgO	Al_2O_3	SiO_2	P_2O_5	K_2O	CaO	TiO_2	Fe_2O_3	MnO	LOI
Site 1R											
Q86-P-57	0.2	1.5	20.1	57.2	0.2	2.4	1.2	1.0	4.4	0.03	11.5
Q86-P-58	0.2	1.5	20.0	58.3	0.1	2.4	1.1	1.0	4.1	0.03	11.2
Q86-P-59	0.2	1.4	19.5	57.6	0.2	2.3	1.3	0.9	5.1	0.04	10.8
Site 11											
Q86-P-60	0.04	0.2	23.5	52.5	0.1	0.9	0.04	1.7	7.7	0.02	12.9
Q86-P-61	<0.01	0.04	6.4	88.7	0.03	0.2	0.03	0.7	0.8	0.02	3.0
Q86-P-62	<0.01	<0.01	2.0	96.0	0.02	0.1	0.01	0.6	0.4	0.02	0.9
Q86-P-63	<0.01	0.1	16.4	66.0	0.04	0.7	0.01	1.4	7.0	0.02	7.5
Q86-P-65	0.1	0.9	16.6	46.4	0.6	1.9	2.3	0.8	16.5	0.1	13.2
Q86-P-66A	0.2	1.0	18.2	50.1	0.4	2.0	2.5	0.9	11.2	0.1	13.1
Q86-P-66B	0.1	0.9	15.3	42.5	0.2	1.7	1.2	0.8	14.5	0.2	22.8
Q86-P-67A	0.2	1.1	20.1	49.9	0.1	2.2	4.6	0.9	5.7	0.2	14.1
Site 17											
Q86-P-69	0.8	0.6	8.3	77.6	0.1	1.5	0.6	0.8	3.4	0.1	6.2
Site 15											
Q86-P-72	0.6	0.8	11.1	68.6	0.1	1.7	0.7	0.9	6.3	0.3	8.2
Q86-P-74	0.1	0.04	2.1	47.0	0.4	0.7	1.2	0.2	31.2	1.8	15.5

Table 2(b)
Major Element Oxide Concentrations (Weight %)
(Purus River Sites)

	Na_2O	MgO	Al_2O_3	SiO_2	P_2O_5	K_2O	CaO	TiO_2	Fe_2O_3	MnO	LOI
89-A-1	0.5	1.1	19.5	55.1	0.1	2.4	4.3	0.8	5.4	0.08	8.3
89-A-2	0.6	1.0	17.8	58.0	0.4	2.4	3.1	0.8	7.2	0.06	11.0
89-A-3	0.5	1.1	19.0	64.0	0.2	2.5	0.9	0.8	5.9	0.04	4.1
89-A-4	0.5	0.9	17.5	61.3	0.2	2.2	2.1	0.7	6.0	0.04	7.3
89-A-5	0.5	1.0	18.6	67.2	0.2	2.3	0.8	0.7	7.1	0.05	6.0
89-A-6	0.6	0.5	8.5	90.0	0.08	1.4	0.3	0.6	3.3	0.05	2.0

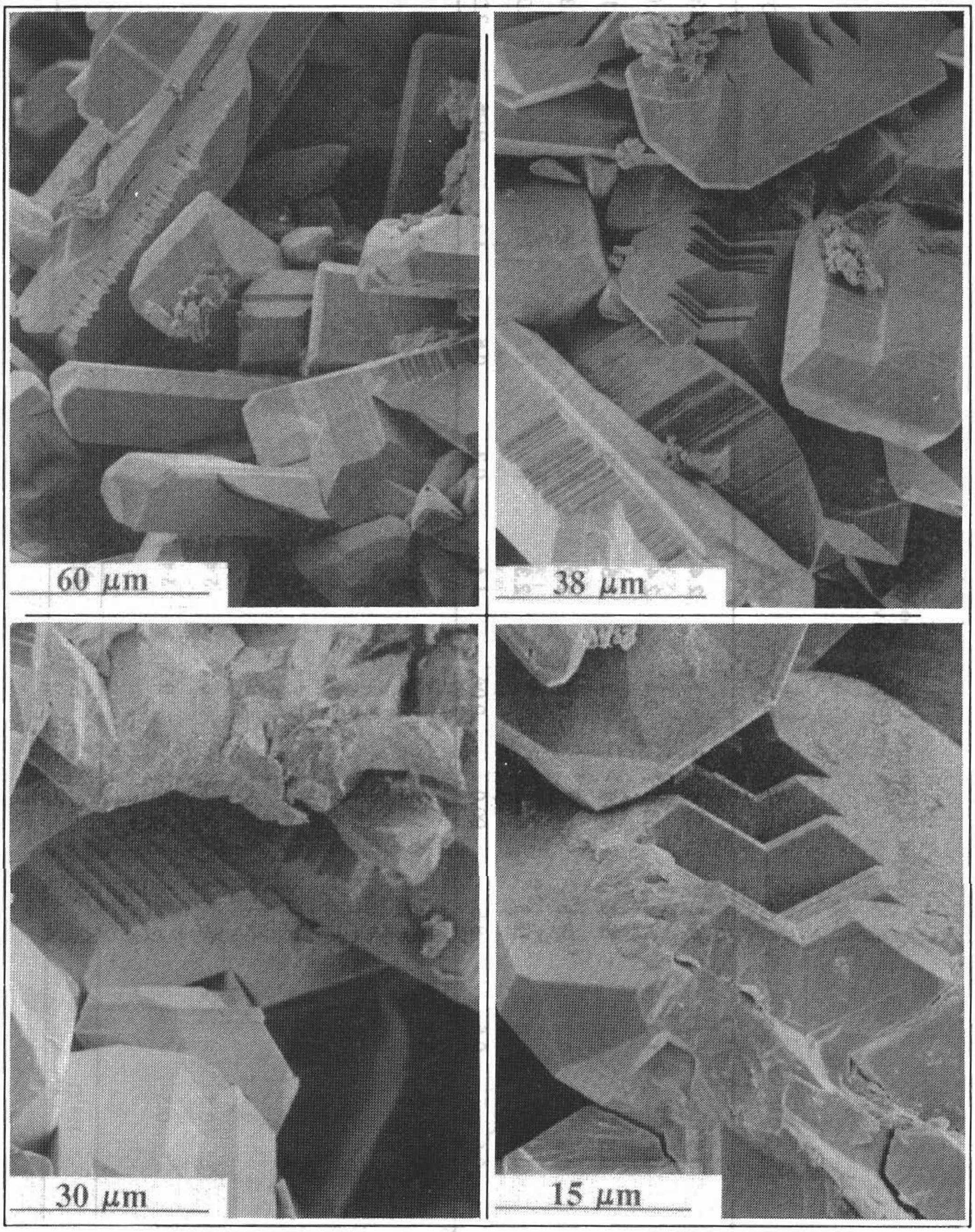

Figure 3 - SEM photos of aragonite crystalllites indicative of gradual precipitation (Photos by A. Mackenzie)

Table 3(a)
Minor Element Concentrations (Weight %)
(Purus River Sites)

Sample	Cr	Rb	Sr	Y	Zr	Nb	Ba	CIA
Site 1								
Q86-P-6	140	120	80	30	260	30	530	85
Q86-P-7	70	150	150	40	160	20	550	86
Q86-P-8	140	90	80	30	830	20	550	63
Q86-P-9	<70	150	100	30	230	20	600	84
Q86-P-10	<70	180	120	40	180	30	560	86
Q86-P-11	<70	160	130	40	160	30	570	85
Q86-P-12	70	<10	<10	<10	140	40	470	83
Q86-P-12A	<70	50	2900	10	30	10	80	
Q86-P-13	70	173	138	24	179	34	596	86
Q86-P-14	70	169	148	18	160	27	574	86
Q86-P-15	<70	152	140	44	172	20	482	86
Site 2								
Q86-P-16	270	<10	<10	<10	490	30	330	89
Site 3								
Q86-P-17	70	<10	10	<10	890	10	1010	
Site 4								
Q86-P-18C	<70	<170	140	20	230	30	770	84
Q86-P-19	<70	20	5060	<10	<10	10	<10	
Q86-P-20	70	90	60	40	400	20	450	86
Q86-P-21	<70	110	340	70	360	20	640	89
Q86-P-22	70	100	40	50	440	30	460	85
Q86-P-23	<70	170	140	40	230	30	610	84
Q86-P-24	<70	170	170	20	180	20	530	86

Cont.

Sample	Cr	Rb	Sr	Y	Zr	Nb	Ba	CIA
Site 5								
Q86-P-25	140	<10	10	<10	570	20	420	
Q86-P-27	<70	<10	<10	<10	<10	40	420	81
Site 7								
Q86-P-30	<70	40	100	10	40	<10	70	
Q86-P-31	<70	160	130	20	230	20	730	86
Q86-P-32	140	<10	20	20	510	30	450	84
Q86-P-33	<70	178	151	18	179	30	637	85
Q86-P-34	70	152	153	52	192	16	643	84
Q86-P-35	<70	174	141	26	149	21	718	86
Q86-P-36	<70	154	121	32	203	45	826	85
Q86-P-37	<70	60	660	530	90	20	380	
Q86-P-40	270	130	100	40	160	20	460	86
Site 8								
Q86-P-44	<70	107	69	62	309	27	400	75
Q86-P-45	200	60	70	50	1460	30	490	58
Q86-P-46a	70	60	20	20	560	30	500	60
Q86-P-46b	<70	<10	<10	<10	142	14	419	74
Site 9								
Q86-P-49	140	<10	70	270	200	30	440	82
Site 10								
Q86-P-51	<70	175	179	38	168	21	645	84
Q86-P-53	<70	151	194	47	208	28	438	83
Site 1R								
Q86-P-57	<70	165	143	39	162	21	547	86
Q86-P-58	<70	174	151	36	176	29	557	86
Q86-P-59	<70	162	147	34	177	23	522	86

Cont.

Sample	Cr	Rb	Sr	Y	Zr	Nb	Ba	CIA
Site 11								
Q86-P-60	70	70	40	50	560	50	340	95
Q86-P-61	140	40	<10	30	510	20	180	96
Q86-P-62	140	10	<10	10	420	20	120	93
Q86-P-63	70	40	20	40	610	50	340	95
Q86-P-65	<70	140	70	30	160	20	490	87
Q86-P-66A	<70	160	110	30	170	40	600	86
Q86-P-66B	70	140	80	50	160	10	530	87
Q86-P-67A	<70	160	150	60	140	20	670	87
Site 17								
Q86-P-69	200	70	80	60	690	20	540	65
Site 15								
Q86-P-72	140	100	90	70	520	20	590	74
Q86-P-74	200	<10	<10	<10	80	20	410	

The commonly observed carbonate and gypsum deposits would have formed as lake waters concentrated sufficiently to precipitate these pahses. Calcium (Ca^{2+}) and bicarbonate (HCO^-_3) ions generally make up 60-70% of the dissolved inorganic component of fresh waters and, thus, $CaCO_3$ phases will be the dominant precipitates resulting from the concentration of lake waters. Gypsum ($CaSO_4.2H_2O$) has a solubility product ~4 orders of magnitude lower than that of aragonite and would precipate in the final stages of desiccation as observed in modern arid regions. The percent levels of S in the lake bed sediments analyzed in this (Table 3b) suggest that S released during the oxidation of bioorganic matter in the desiccating lake floor would have been an additional source of sulphate ions from the evaporating lake waters. (Further evidence of diagenetic biological activity on the active lake floor comes from the presence of siderite replacing bone tissue, Benchimol **et al.**, 1987) and as a major phase in ''conglomerate'' samples (Q86-P-25, 27, 49). Siderite is a common product of anaerobic diagenetic processes in lake sediments and precipitates from interstitial waters ~20-30 cm below the lake sediment surface (Emerson, 1976). The radiocarbon ages of samples of aragonite and biological debris entrained in the clay (lake bed) sediments suggest that the lake, represented in the surficial Acre Basin sediments (Solimoes Formation), desiccated in the latter part of the last glacial cycle (LGC). $CaCO_3$ deposition would suggest that regional evaporation rates had exceeded those of fresh water fluxes into the lake from the atmosphere and from ground and stream waters. The extensive distribution of gypsum deposits throughout the Acre Subbasin are direct evidence that the declining inputs of water eventually led to aridity and this is the first direct evidence for arid climate conditions in Amazonia during the LGC.

It is also likely that arid climate conditions may have been confined to Western Amazonia. The modern Amazonian hydrological cycle is recharged by moisture derived mainly from air masses entering Amazonia from the Atlantic Ocean, and the modern rainforest play a significant role in evapotranspirational recycling of rainwaters across the basin (Salati & Vose, 1986). If the Atlantic Ocean circulation patterns were different during the LGC (Broecker, 1989) and if global sea surface temperatures were depressed by 2-4°C (Rind & Peteet, 1985), then the Atlantic Ocean moisture fluxes into Amazonia would have been diminished, thereby disrupting the rainforests in eastern and central Amazonia (Prance, 1982) and resulting in aridity in western Amazonia. (Even under present climate conditions western Amazonia experiences definite dry periods (Salati & Vose, 1986).

There is tentative evidence, from the age dates at the Acre River site, that the desiccation of lake waters occurred over several millenia. Here the age (49,110 ± 900 a BP) of one of the aragonite concretions found ~4 m below the uppermost clay sediments could represent the time at which the lake waters concentrated

Table 3(b)
Minor Element Concentrations ($\mu g g^{-1}$) and CIA Values
(Acre River Sites)

	S	V	Cr	Co	Cu	Zn	Sr	Y	Zr	Nb	Mo	Ba	Pb	CIA
89-A-1	0.7(%)	121	76	37	72	100	222	23	85	11	5	530	65	82
89-A-2	1.2(%)	136	70	24	37	112	192	29	92	12	7	450	65	81
89-A-3	335	121	77	26	50	110	114	18	88	10	4	540	63	81
89-A-4	0.7(%)	112	70	22	44	110	116	21	96	10	2	400	60	81
89-A-5	136	126	74	22	35	105	115	16	86	10	3	460	64	81
89-A-6	44	65	35	15	15	52	67	14	80	8	-	350	30	71

BELOW DETECTION

sufficiently to precipitate $CaCO_3$ phases. The relatively high concentrations of Ca in the sediments (89-A-1, A-2; Table 2b) enclosing the concretions suggest that the concretions are likely in situ. (The intricate crystallite patterns (Figure 3) observed using scanning electron microscopy are consistent with very slow rates of $CaCO_3$, nucleation and precipitation). If we assume that the virtually complete reptilian skeletons in the uppermost clay sediment layers congregated at a local pond during the final stages of lake desiccation, the radiocarbon age date (23,950 ± 420 a BP) from a sample of reptilian skeleton may represent the time frame for the final stages of desiccation. The long time period for the desiccation of the proposed lacustrine system may be consistent with cooler climates (Kam-biu & Colinvaux, 1985) and the possibility that the LGC lacustrine system was very large, as suggested from the drill core samples (Kronberg **et al.**, 1989) by a 60 m clay unit underlying a calcareous sediment unit dated at 13,390 ± 90 a BP. (Other circumstantial evidence for a gigantic lacustrine system comes from fossils of gigantic reptiles commonly found enclosed in the clay sediments of the Acre Basin (e.g. Couto, 1960).

The evidence for aridity in Western Amazonia is important in establishing boundary conditions for LGC climate models and in indicating the extent to which the global hydrological cycle was influenced by vast fresh water transfers to the cryosphere as alpine glaciers advanced and continental ice sheets accumulated in polar and temperate latitudes. (Table 4a) and of wood samples (as yet unidentifies) with radiocarbon dates in the 40,000 a BP range (Table 4a).

The evidence for aridity in Western Amazonia is important in establishing boundary conditions for LGC climate models and in indicating the extent to which the global hydrological cycle was influenced by vast fresh water transfers to the cryosphere as alpine glaciers advanced and continental ice sheets accumulated in polar and temperate latitudes. Drier, cooler Amazonia climates during the LGC would be consistent with the

Table 4(a)

	SAMPLE DESCRIPTION (sample identification)	AGE (radiocarbon yeras)
Purus River Sites		
4	aragonite concretion	53,270±1,850
	(Q86-P-19)	
4	fossil wood	
	(Q86-P-18A,B)	>25,000
7	fossil wood	
	(Q86-P-43)	45,180±690
10	fossil seed	32,160±230
	(Q86-P-56)	
	Swartzia polyphyllea Dc.	
15	fossil wood	45,190±830
	(Q86-P-68)	
Acre Riiver Sites		
1	aragonite concretion	49,110±900
	(89-A-Ca)	
1	fossil wood	41,850±490
	(AMM-89)	
1	fossil reptilian bone	23,950±420
	(Q89-A-B)	
Rio Branco	fossil wood	11,870±70
	(Kronberg-1)	
Purus River	fossil turtle bone	12,060±150
(collected prior to 1986)	(Kronberg-2)	
	fossil crocodile claw or tooth	24,130±330
*	(Kronberg-3)	

* Accelerator mass spectrometric (AMS) radiocarbon analyses by Dr. R.P. Beukens, ISOTRACE, University of Toronto, Canada

Table 4(b)

Sample Number	$\delta^{13}C$	$\delta^{18}O$	$\delta^{18}O$	$^{87}Sr/^{86}Sr$
	(vs. PDB)	(vs. SMOW)	(vs. PDB)	
89-A-Ca (Acre River)	-12.54	+25.05	-5.68	
Q86 P-19 (Purus River)	-18.05	+24.70	-6.02	0.70999
Q86 P-30 (Purus River)				0.71003

evidence summarized by Schubert (1988) for drier, cooler LGC climates in northern South America and the Caribbean.

The direct evidence for aridity in Western Amazonia documented here also raises questions regarding the evolution of the modern Amazonian mosaic of rainforests as well as the role of the Amazonian and other tropical rainforests in the global carbon, hydrological and energy cycles (Kronberg & Fyfe, 1990; Shukla **et al.**, 1990).

ACKNOWLEDGEMENTS

This research was funded by the Brazilian Departamento Nacional de Produção Mineral (DNPM), the National Institute for Amazonian Research (INPA) and the Canadian Natural Sciences and Engineering Research Council (NSERC). Sociedade Fogás Ltda. (Manaus), Dr. Saul Benchimol (Manaus) and Sr. Francisco de A. P. da Silva (Rio Branco) provided invaluable field and logistical support. Ana Emmelinda a Aldeniza (Universidade do Amazonas), and Ricardo (Universidade do Acre) are acknowledged for assisting with sample collection. Luiz Fernandes Coelho (INPA) provided the name of the plant species from which a fossil seed would have originated. M. I. Bird and R. H. McNutt are achnowledged for providing C and O isotope data respectively. S. Spivak and S. Millar are acknowledged for assistance in the preparation of the manuscript. This research is a contribution to IGCP project 281 - Quaternary Climates of South America.

SUMMARY

As análises geoquímicas e geocronologicas de amostras superficiais de sedimentos e fósseis encontrados no norte da bacia do Acre, indicam um sistema extensivo fluvio-lacrustrino ocupando esta região dissecando lentamente durante o último ciclo glacial (LGC). Esta pesquisa documenta evidência direta para aridez na Amazônia Ocidental no Quaternário, e é importante no estabelecimento de condições dos limites para os modelos climáticos para o LGC como também na corelação entre as condições climáticas (LGC) marinhas e continentais.

References

Asmus, H. E. & Porto, R. - 1972. Classificação das bacias sedimentares brasileiras segundo a tectônica de placas. **Anais Congresso Brasileiro de Geologia,** 26(2):67-90.

Benchimol, R. E.; Cooper, K.; Kronberg, B. I.; Powell, M. - 1987. Reconnaissance study of macrofossils from the Upper Purus River, Western Amazonia. **Acta Amazonica,** 16-17:327-336.

Broecker, W. S. & Denton, G. H. - 1989. The role of ocean-atmosphere reorganizations in glacial cycles. **Geochim. et Cosmochim. Acta,** 53:2465-2501.

Couto, C. de P. - 1960. Uma preguiça terrícola da região do Alto Amazonas, Colômbia. **Bol. Mus. Nacional (Rio de Janeiro),** 31:1-9.

Emerson, S. - 1976. Early diagenesis in anaerobic lake sediments: chemical equilibria in interstitial waters. **Geochim. et Cosmoschim. Acta,** 40:925-934.

Fairbridge, R. W. - 1972. **The encyclopedia of geochemistry and environmental sciences.** 2nd edition, Van Nostrand, New York. 1321 p.

Kam-biu, L. & Colinvaux, P. - 1985. Forest changes in the amazon basin during the last glacial maximum. **Nature,** 318:556-557.

Kronberg, B. I. & Nesbitt, H. W. - 1981. Quantification of weathering, soil geochemistry and soil fertility. **J. Soil Sci.,** 32(3):453-459.

Kronberg, B. I.; Nesbitt, H. W.; Lam, W. - 1986. Upper pleistocene amazon deep-sea fan muds reflect intense chemical weathering of their mountainous source lands. **Chem. Geol.**, 54:283-294.

Kronberg, B. I.; Benchimol, R. E.; Hazenberg, G.; Doherty, W.; VanderVoet, A. - 1989. Geochemical variations in Solimões Formation sediments (Acre Basin, Western Amazonia). **Acta Amazonica**, 19:319-333.

Kronberg, B. I. & Fyfe, W. S. - 1990. Forest-climate interactions: implications for tropical and boreal forests. **J. Bus Admin.** (in press).

Miura, K. - 1972. Possibilidades petrolíferas da bacia do Acre. **In: Anais Congresso Brasileiro de Geologia**, 26, Belém v. 3, p. 15-20.

Prance, G. T. (ed.) - 1982. Biological diversity in the tropics. Columbia University Press, New York. 714 p.

RADAMBRASIL - 1978. Levantamento de recursos naturais (geologia, geomorfologia, pedologia, vegetação, uso potencial da terra). Folha SB. 19 Jurua, v. 15. Rio de Janeiro, Departamento Nacional da Produção Mineral. p. 55-58.

Rego, L. F. de M. - 1930. Notas sobre a geologia do território do Acre e da Bacia do Javari. 45 p.

Rind, D. & Peteet, D. - 1985. Terrestrial conditions at the Last Glacial Maximum and CLIMAP sea surface temperature estimates: are they consistent? **Quat. Res.**, 24:1-22.

Salati, E. & Vose, P. B. - 1984. Amazon Basin: a system in equilibrium. **Science**, 225:129-138.

Santos, J. O. S. - 1984. A parte setentrional do Craton Amazônico (Escudo das Guianas) e a Bacia Amazônica. **In: Geologia do Brasil**. (eds.) Schobbenhaus, C.; Campos, D. A.; Derze, G. R.; Asmus, H. E.

Brasília, DNPM. 501 p.

Schubert, C. - 1988. Climatic changes during the last glacial maximum in northern South America and the Caribbean: a review. **Interciencia**, 13(3):128-137.

Shukla, J.; Nobre, C.; Sellers, P. - 1990. Amazon deforestation and climate change. **Science**, 247:1322.

(Aceito para publicação em 24.09.1991)